Questioning the existence of ultra high-frequency seismic waves based on DEM analysis of gate columns

Radan Ivanov *, Shiro Takada **

* Ph.D., Visiting Researcher, Dept. of Eng., Kobe University, 1-1, Rokkodai, Nada-ku, Kobe-shi, 657-8501
** Dr. of Eng., Professor, Dept. of Eng., Kobe University, 1-1, Rokkodai, Nada-ku, Kobe-shi, 657-8501

In this paper, qualitative evaluation of the potential for jumping of column crowns under several types of dynamic disturbances is performed. It was found that typical vertical earthquake motion cannot cause notable separation at the column-crown interface. Substantial separation could occur due to short velocity pulses as well as earthquake waves of exceptionally high frequency and huge peak accelerations. However, our numerical results as well as experiments done by others indicate that the effect of pulse input would not be limited to flying off of crown but will as well cause either significant structural damage to the column in the form of tensile cracks that spread over the entire cross section, or pulling of the column together with the footing out of the ground. Discovery of such damage modes in post-earthquake surveys could serve as indirect proof of the existence of ultra high-frequency seismic waves.

Key Words: jumping, high-frequency waves, discrete element method

1. Introduction

Reportedly, there are witness observations indicating that during strong earthquakes objects fly off the ground reaching notable heights. Although not substantiated by hard evidence there must be some truth in such statements which renders a quantitative study on what height a body not firmly fixed to its base can reach when subject to various types of dynamic disturbances and earthquake waves in particular. One plausible reason for occurrence of fly-off is the possible existence of seismic waves of very high frequency and acceleration amplitude that due to the limitations of present day earthquake recording equipment remain unnoticed in the accelerograms. Certain observed failure modes of structures during earthquake could be attributed to the existence of such undetected waves, e.g. circumferential cross sectional cracking of RC bridge piers or elephant foot buckling mode of steel bridge piers during the 1995 Kobe earthquake. These two cases were experimentally studied by Ishikawa and Mori[1), 2)] on scaled models. The circumferential cracking for instance was successfully simulated on input of a wave with peak acceleration 400m/s^2 and predominant frequency 24.4Hz. After scaling-up the results to the original structure they obtained the parameters of the likely destructive waves as peak acceleration about 12m/s^2, peak velocity about 1.2m/s and predominant frequency 0.8Hz and 1.6Hz for the RC and steel piers respectively. Obviously such waves are within the resolution capability of typical accelerometers and would have been detected if a measurements were taken on the particular sites during the earthquake. The fact that the above failure modes are realized for typical earthquake waves means that they cannot be considered as evidence for the existence of undetectable ultra high-frequency earthquake waves. Hakuno[3)] suggests that it is the frequency incompleteness of earthquake records that fails us to explain the surprisingly low level of damage associated with the very strong records of peak acceleration exceeding 10m/s^2 and velocities near 3m/s e.g. Northridge – 18.4m/s^2, Tottori – 14.8m/s^2, Taiwan – velocity around 3m/s. Izumi[4)] draws our attention to a number of earthquake associated phenomena that could be linked to ultra-high frequency waves; ground liquefaction, fly-off of objects, occurrence of engine trouble of ships due (probably) to the transmission of P-waves through water, compression or tension failure of structural members loaded axially (columns, piles etc.). If we add to this the still not very clear nature of earthquake mechanisms the question of existence of ultra-high frequency waves in earthquakes records seems wide open. In what follows we concentrate on the fly-off of column crowns of front gate columns in Japanese houses and try to establish the effects of vertical motion input to their bases. We chose this particular structure because it is simple, widespread and relatively uniform in scale, design and construction throughout Japan. Our strategy is to quantify its behavior by numerical experiments so that if similar behavior patterns are observed during earthquake these to be judged as the result of input ground motion similar to those we used in the numerical experiments.

2. Mechanical model

The most straightforward approach to roughly evaluate the height a body can reach is to analyze the motion of a mass point. Consider a mass point sitting on top of a base point. If the base point is moved upwards with velocity v_o and then instantaneously stopped, the mass point will fly off with the same velocity. Then the maximum height H_1 it can reach in the presence of gravity is,

$$H_1 = v_0 t - \frac{gt^2}{2} \tag{1}$$

Solving this equation for various initial velocities we can obtain the corresponding maximum heights. The results for maximum height are shown in Fig.1, and the time histories

of vertical motion in Fig.2. It is obvious that even in the case of a relatively high initial velocity of 1.5m/s the maximum height is in the order of 0.1m. In obtaining the above results it is assumed that the base point from which we measure the maximum heights does not move while the mass point is in motion. During earthquake this is not the case and the apparent hight defined as the distance betweeen the base point and the flying point will vary depending on the particular earthquake record. Thus, if the velocity of the base immediately after fly-off continues to be in the upward direction the apparent height will be smaller than the height predicted by Eq.(1). On the contrary, if the velocity of the base changes direction after fly-off the apperent height will be greater. It is wortwhile considering a worst case scenario where upon reaching upward velocity v_o equal to the peak velocity of an earthquake record the base immediately starts a downward motion with the same velocity. In this case a height $H_2=v_0t$ has to be superimposed to H_1 from Eq.(1) and the apparent height will be,

$$H = H_1 + H_2 = 2v_0 t - \frac{gt^2}{2} \qquad (2)$$

Comparing Eqs.(1) and (2) we see that the apparent height given by Eq.(2) could reach a value of twice the flight height given by Eq.(1). The maximum apparent height for a particular velocity can then be found by doubling the maximum flight height corresponding to that velocity. We think the technique proposed above will give an upper bound of the maximum apparent height provided the amplification factor for velocity is not too large, i.e. the structure on which the body stands is stiff enough to be considered rigid. Should this be the case Eq.(2) will always give conservative values for the apparent height. The reason why Eq.(2) is always conservative in the absence of dynamic amplification is that the structure is flexible so before the body can fly off the compressive stress at the interface has to become zero. Both the effect of dynamic amplification and the effect of flexibility cannot be considered using the present mass point model. Their influence will be discussed in the following paragraph.

The vast data base of recorded earthquake waves around the world in the past indicates that the peak vertical velocity of earthquakes rarely exceeds 0.5m/s, so from Fig.1 we can conclude that the maximum apparent height due to earthquake motion can be expected to be in the order of 0.05m (twice the value from the chart).

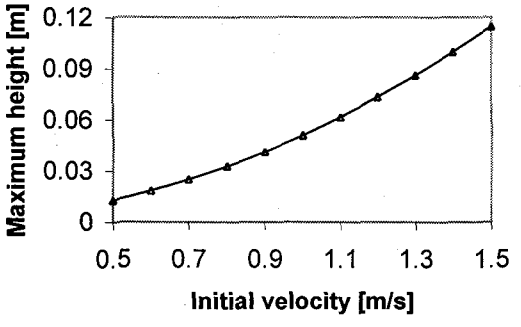

Fig.1 Maximum flight heights

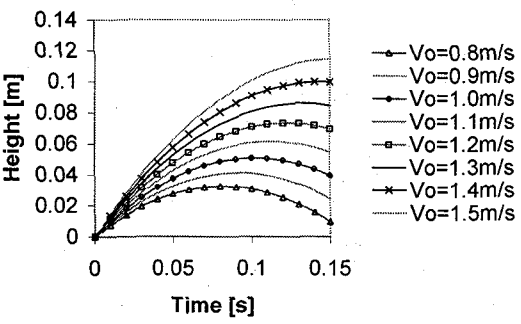

Fig.2 Time histories of flights

3. Numerical evaluation

As mentioned in the previous paragraph the influence of the effects of dynamic amplification and flexibility has to be evaluated in order to confirm the reliability of the mass point model. To this end, a 1.8m high concrete column with a cross section of 0.18m^2 (0.42m/0.42m) was used as the base of a concrete body with dimensions 0.5m/0.5m/0.1m. The Young's modulus of conrete used was assumed 2.4x10^{7}kN/m2. This structure corresponds to the column of a front gate to a typical Japanese family house with a crown plate on top[5].

3.1 model and solution procedure

A discrete model of lumped masses and springs as shown in Fig.3 was used for the column. The interaction between the crown and the column was modeled by two springs; one compression-only and one tension-only. The tension spring is allowed to break upon reaching a specified value of the force in the spring, so that situations where the joint has finite tensile strength can also be modeled. The compression-only spring on the other hand works any time when the length of the spring becomes smaller than the initial length, so that multiple jumps of the crown and collisions at the column-crown interface can occur during a single run. The column body was modeled by compression-tension springs which were not allowed to break. In view of the expected breaking and large separation at the interface a discrete element solution procedure was employed. The

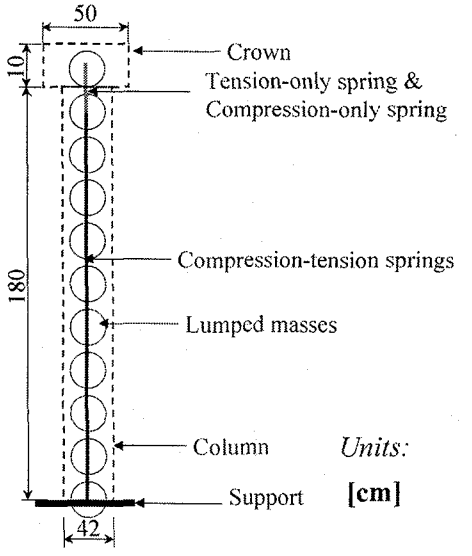

Fig.3 Analysis model

input motion was applied at the support level, which is fully fixed. In what follows, the general interaction of a pair of elements (*i, j*) with an axial spring between them is considered. First we calculate the incremental displacements $\Delta \boldsymbol{x}_i$ and $\Delta \boldsymbol{x}_j$ of the two elements,

$$\Delta \boldsymbol{x}_i = \boldsymbol{v}_i^+ \Delta t, \qquad \Delta \boldsymbol{x}_j = \boldsymbol{v}_j^+ \Delta t \tag{3}$$

where $\boldsymbol{v}_i^+$ and $\boldsymbol{v}_j^+$ are the velocities of elements *i* and *j* respectively and Δt is the time step. Superscripts + and – indicate new and old values respectively. Next we calculate the relative displacement between the two elements $\Delta \boldsymbol{x}_{ij}$ and its normal component $\Delta \boldsymbol{x}_{ij}^n$,

$$\Delta \boldsymbol{x}_{ij} = \Delta \boldsymbol{x}_j - \Delta \boldsymbol{x}_i \tag{4}$$

$$\Delta \boldsymbol{x}_{ij}^n = (\Delta \boldsymbol{x}_{ij} \cdot \boldsymbol{n}_{ij}) \boldsymbol{n}_{ij} \tag{5}$$

where $\boldsymbol{n}_{ij}$ is the unit normal vector pointing from element *i* to element *j*. Then we compute the increment of spring force $\Delta \boldsymbol{F}$,

$$\Delta \boldsymbol{F} = k \Delta \boldsymbol{x}_{ij}^n \tag{6}$$

where k is the spring constant. In addition to the force in the in the spring there is a damping force $\boldsymbol{F}_d$ acting at the interface between elements *i* and *j*,

$$\boldsymbol{F}_d = \eta \Delta \dot{\boldsymbol{x}}_{ij}^n \tag{7}$$

The local damping damping coefficient η is computed for by the formula $\eta = 2\xi\sqrt{km_{av}}$, in which m_{av} is the average of the masses of elements *i* and *j*, and the critical damping ratio ξ=0.05, was used for concrete. The direction of the force in the spring has meanwhile changed, so we first update it to mach the latest normal between the two element centres,

$$\boldsymbol{F}^- = F^- \boldsymbol{n}_{ij} \operatorname{sgn}(\boldsymbol{F}^- \cdot \boldsymbol{n}_{ij}) \tag{8}$$

where $\boldsymbol{F}^-$ is the force in the spring from the previous time-step, F^- its value and sgn( ) designates the sign function (yielding + 1 or -1). Finally we add the increment to yield the provisional updated value of the force in the spring,

$$\boldsymbol{F}^+ = \boldsymbol{F}^- + \Delta \boldsymbol{F} \tag{9}$$

where $\boldsymbol{F}^+$ is the force in the spring at the end of the current time step. The force so calculated is sufficient to carry out elastic analysis. In case of material nonlinearity the force is modified to reflect the adopted stress-strain curve or the spring is taken out of further consideration if its strength (elastic-brittle spring) or ductility limit (elastic-plastic spring) is exceeded. After having been modified, the force in the spring is added to the resultants of forces acting on elements $\boldsymbol{F}_i$ and $\boldsymbol{F}_j$. The damping force is also added,

$$\boldsymbol{F}_i = \boldsymbol{F}_i + \boldsymbol{F}_{mod} + \boldsymbol{F}_d \tag{10}$$

$$\boldsymbol{F}_j = \boldsymbol{F}_j - \boldsymbol{F}_{mod} - \boldsymbol{F}_d \tag{11}$$

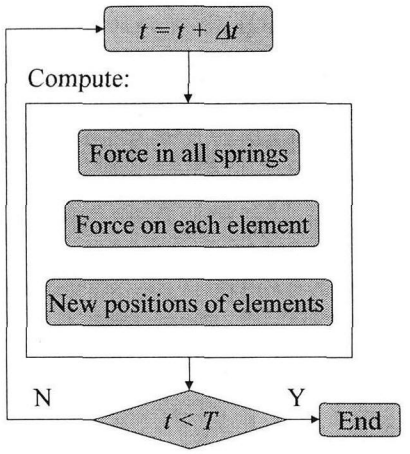

Fig.4 Solution algorithm

where $\boldsymbol{F}_{mod}$ is the modified value of $\boldsymbol{F}^+$. The force resultant of an element receives contributions from all springs connected to that element. The elements are now ready for calculating new positions. The equation for translational motion of a single element is,

$$\ddot{\boldsymbol{x}}_i + \alpha \dot{\boldsymbol{x}}_i = \boldsymbol{F}_i / m_i + \boldsymbol{g} \tag{12}$$

where $\boldsymbol{x}_i$ is the position vector of element *i*, m_i is its mass, and $\boldsymbol{g}$ the gravity acceleration. Integration in time is designated by dots. A centred finite difference is used to integrate the equations of motion. New and old values are designated by superscripts plus and minus. The expression for velocity is,

$$\ddot{\boldsymbol{x}}_i = \frac{1}{\Delta t}\left[\dot{\boldsymbol{x}}_i^+ - \dot{\boldsymbol{x}}_i^-\right] \tag{13}$$

Inserting this expression in the equation of motion Eq.(12) and solving for the new value of the velocity results in,

$$\dot{\boldsymbol{x}}_i^+ = [D_1 \dot{\boldsymbol{x}}_i^- + (\boldsymbol{F}_i / m_i + \boldsymbol{g})\Delta t] D_2 \tag{14}$$

where $D_1 = 1 - (\alpha \Delta t / 2)$, $D_2 = 1/[1 + (\alpha \Delta t / 2)]$. The coefficient of global damping in the analyses was assumed $\alpha = 0$ since the column is surrounded by air. The flow of the solution algorithm is shown in Fig.4. All analyses were performed by a multipurpose DEM program[6].

3.2 Response to earthquake motion

A summary of the analyses carried out is shown in Table 1. The response of the structure to vertical earthquake motion was computed for two real earthquake waves from

Table 1 Summary of analyses

ID	Earthquake wave	Tensile strength at interface [kN/m^2]	Max. separation at interface [m]
A1	Takatori	0.5	2.5x10^{-6}
A2	JMA	0.0	0.0
A3	Takatori	5.0	0.0

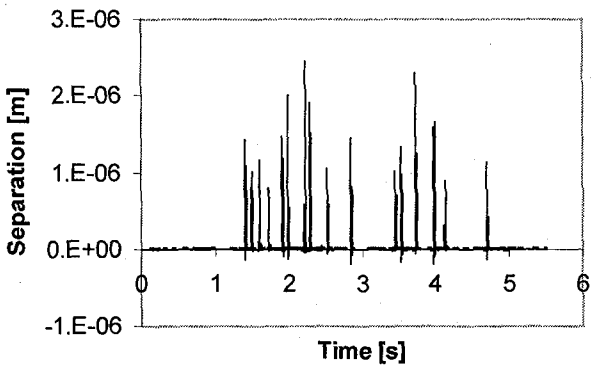

Fig.5 Time history of separation at interface

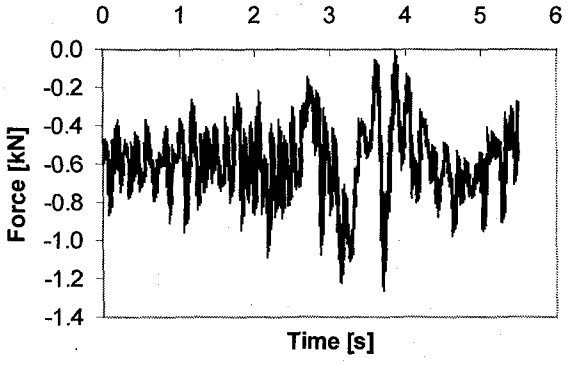

Fig.6 Force at the column-crown interface

the 1995 Kobe Earthquake; JMA with predominant frequency 0.8Hz and Takatori Station with predominant frequency 8Hz. The original amplitudes of the records were scaled up to peak acceleration 8m/s^2. Under these conditions the peak velocities become 0.47m/s and 1.0m/s for the Takatori and JMA records respectively.

The time history of separation distance for A1 is shown in Fig.5. Several jumps and collisions occur through the run but the maximum separation distance is negligibly small.

In analysis A2 the force at the interface link remains compressive throughout, so separation does not occur, see Fig.6.

In analysis A3 a slightly larger but still very small bond strength at the interface was applied with all other conditions identical to A1. Even this small strength appears enough to keep the crown from flying off as breaking does not occur at the interface.

On comparing analyses A1 and A2 we notice that even though the peak velocity of the Takatori record is smaller than that of the JMA record, larger flying-off occurs for this record. The reason for this is to do with the frequency content of the records. The Takatori record contains strong high frequency components, so the shift between positive (upward) and negative velocities (downward) velocities is much faster thus allowing the crown to fly-off. In addition the higher frequency record is expected to produce a higher dynamic amplification factor for the velocity of the crown, because the natural frequency of the column is rather high, about 400Hz, so a high frequency record will always be more likely to cause dynamic amplification. Indeed, the results of A2 and A3 indicate amplification factors for velocities 1.0008 and 1.012 for the JMA and Takatori records respectively. Both values are so small that the

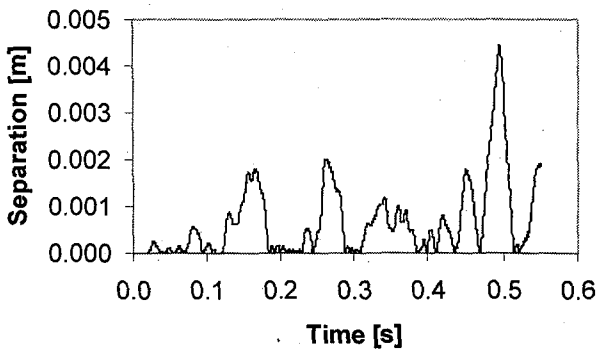

Fig.7 Separation at interface – 80Hz wave

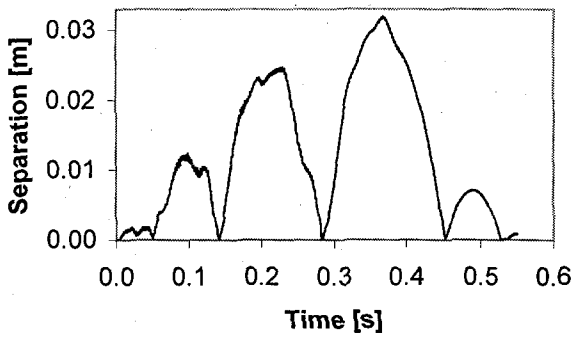

Fig.8 Separation at interface – 400Hz wave

column-crown assembly can be assumed to move as a rigid body when subject to recorded earthquake motion.

3.3 Response to high frequency and pulse input

(a) Earthquake-like input

As confirmed in paragraph **3.2** earthquake motion as recorded by conventional measuring equipment does not produce notable separation between column and crown. Then the reported large separations (if true) must have some other origin. Hypothetically, there could be very short pulses of large amplitude or trains of high-frequency waves not detectable by equipment that could cause large separations to occur. Hereon, we analyse the consequences of such a hypothesis. First, the response of the structure to high frequency earthquake-like disturbance was studied. To this end two waves were produced from the Takatori record by reducing its sampling time-step to 0.001s and 0.0002s resulting in waves of predominant frequency 80Hz and 400Hz respectively. In order to keep the velocity amplitudes the same as those of the original record the acceleration amplitudes were scaled-up accordingly. Thus, the peak accelerations of the two waves became 80m/s^2 and 400m/s^2 respectively. The time-histories of the separation distance at the interface for these two waves are shown in Fig.7 and Fig.8 respectively. Evidently, with increasing frequency of the input wave the separation at the interface increases. The dynamic amplification for velocity in the case of the 80Hz wave is 1.019 and 2.56 for the 400Hz wave. On one hand we see that the amplification factor barely changes between 8Hz and 80Hz input. The larger separation distance produced for

80Hz is only due to the faster alteration between positive and negative velocity. On the other hand the large amplification factor for 400Hz is due to resonance since this is very close to the natural frequency of the structure. Even then we see that the value predicted by Eq.(2) (0.05m) is not reached. This is because given the relatively random nature of an earthquake signal it is very unlikely that jumping occurs exactly at the point of peak velocity. It is much more likely, as shown in Fig.8 that separation will occur at the first possible occasion and following jumps will occur only on collisions which do not need to be at peak velocity. Finally, if we take a more practical view point, the crown will hardly jump several times during earthquake but would rather fall down after the first jump since in fact there is also horizontal ground motion not considered in the present analysis. All the above arguments are deemed enough to conclude that Eq.(2) is sufficient for simple and practical evaluation of the maximum possible separation distance for a given earthquake. The only parameter we need to know is the peak velocity of the earthquake which is easily accessible.

(b) Pulse input

The response of the structure to two types of velocity pulses, constant and triangular was analysed. Summary of the analyses is shown in Table 2.

Table 2 Summary of input data for pulse analyses

ID	Type	Duration - T [s]	Peak velocity [m/s]	Tensile strength at interface [kN/m^2]
P1	constant	0.001	1.0	0.0
P2	constant	0.001	2.0	0.0
P3	constant	0.001	3.0	0.0
P4	constant	0.001	1.0	750
P5	constant	0.001	1.0	2400
P6	triangular	0.002	1.0	0.0
P7	triangular	0.01	1.0	0.0
P8	triangular	0.02	1.0	0.0

The results for maximum separation of P1, P2 and P3 are shown in Fig.9. The dynamic amplification for these three analyses was 2.1, well consistent with the value of 2.0 for the case of reflection of a short longitudinal pulse at the free end of a bar stipulated by wave theory. Thus, the crown flies-off with velocity 2.1m/s, 4.2 m/s and 6.3m/s for cases P1, P2 and P3 respectively.

The effect of the tensile strength at the interface on the fly-off velocity is studied next. When the interface has some

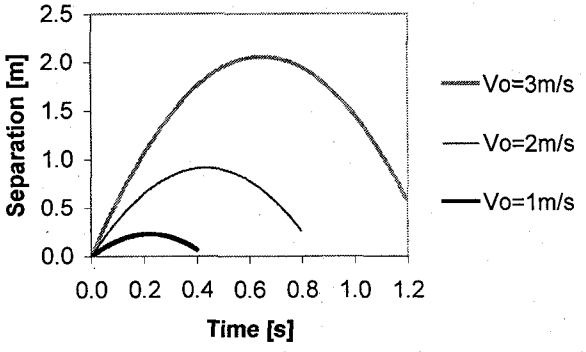

Fig.9 Time-histories of separation – P1, P2 and P3

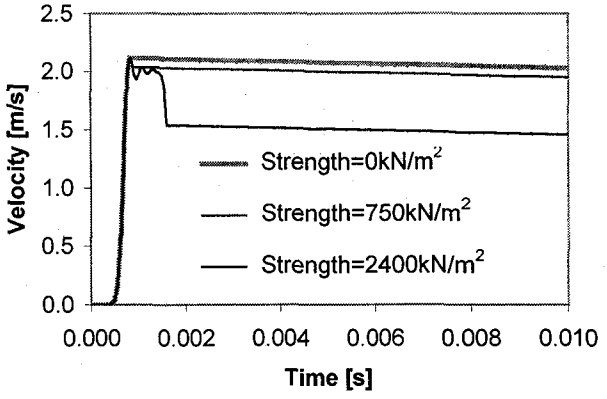

Fig.10 Fly-off velocity of crown depending on strength of interface

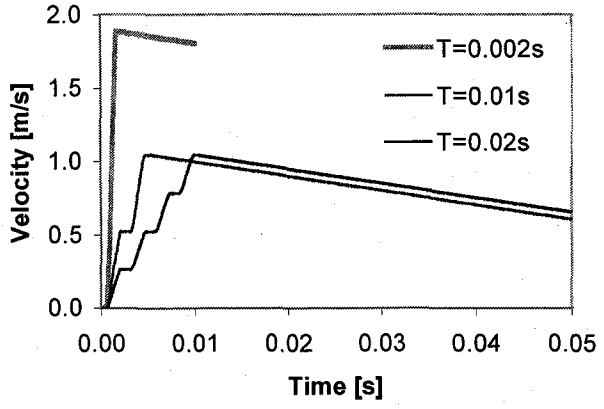

Fig.11 Fly-off velocity of crown depending on pulse duration

strength, breaking will occur only after some potential energy has developed at the interface so certain drop in the fly-off velocity is expected. This effect is shown in Fig.10, where the results from P1, P4 and P5 are plotted . In this figure failure of the interface and subsequent fly-off occurs at the points where the velocity time-history becomes a slightly declining straight line. The value 2400kN/m^2 is a typical tensile strength for concrete so the figure gives us some idea as to by how much the fly-off velocity can be reduced if the interface has some strength.

Finally the response to triangular pulses and the influence of pulse duration is studied. The results for cases P6, P7 and P8 are shown in Fig.11. We see that for short rise time (half the duration) the amplification factor is quite large, and in the limit would reach the value 2.1 yielded by cases P1 to P3. On the other hand as duration increases the amplification factor decreases and for duration 0.01s is effectively unity.

(c) Effects of high-frequency and pulse input on structural performance

So far our discussion has been limited to the ability of various dynamic disturbances to cause flying-off of the crown. It was found so far that only high frequency and pulse input can cause appreciable separation. As it is virtually impossible to record (e.g. take a picture) of an object having been made to fly during earthquake, it would be useful to pinpoint some indirect evidence to tell us that

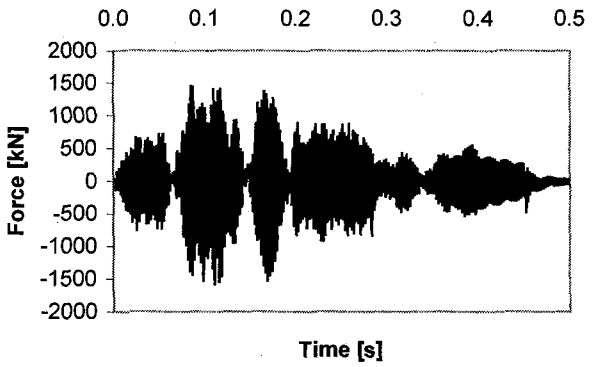

Fig.12 Reaction force due to the Takatori 400Hz wave

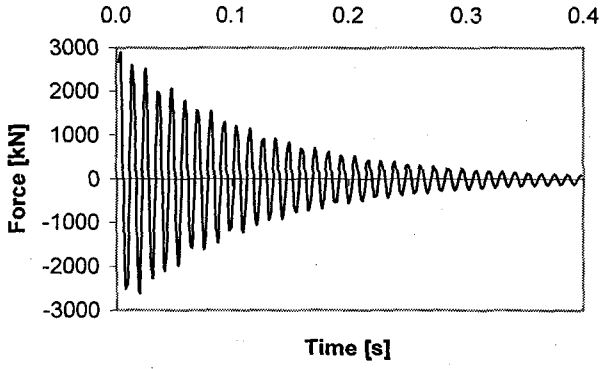

Fig.13 Reaction force due to pulse P1

flying has actually occurred. The time history of the vertical support reaction for the Takatori 400Hz wave and pulse P1 are shown in Fig.12 and Fig.13 respectively. The weight of the whole structure together with the footing is about 25kN. Then the development of a tensile reaction force in the order of 1500kN~3000kN implies that the whole structure will jump-up if friction with the surrounding soil is not enough to prevent this. On the other hand if soil-structure friction is sufficiently large, then a substantial tensile force will work at the section immediately above the footing. A tensile force of 1500kN would produce tensile stress of 8333kN/m^2 in the column, much exceeding the typical tensile strength of concrete, 2400kN/m^2, meaning that cracks parallel to the cross section would appear for both the Takatori 400Hz wave and the P1 pulse input. Gate columns are usually reinforced by four 16mm bars with total area $8x10^{-4}m^2$. Considering steel with yield stress $2.94x10^6$kN/m^2 the bars would yield if the tensile force exceeds 2363kN, i.e., for pulse input P1 the bars will definitely yield. So, it can be concluded that the presence of tensile cracks traversing the whole cross section of the column, or uplift of the column together with the footing could serve as indirect evidence that flying-off has occurred during earthquake. The uplift criterion should be used with care since it could be influenced by liquefaction of the surrounding ground.

4. Conclusions

(1) Earthquake motion as recorded by instruments cannot cause appreciable separation at the column-crown interface.

(2) High-frequency disturbances of above about 200Hz could cause significant separations. However, these would be accompanied by side effects such as jumping-up of the whole structure out of the ground, or large circumferential tensile cracks. Unless some of these side effects are spotted on site it cannot be concluded that very high frequency components have existed in the record.

(3) The presence of high-frequency components is a necessary but not sufficient condition for occurrence of a notable fly-off. As demonstrated by the analyses using high-frequency earthquake-like input separation occurs at the first possible occasion before reaching the potentially most powerful part of the record. So, statistically speaking the chances of a collision to coincide in time and phase with the beginning of a segment of the record that can cause high fly-off are relatively small.

(4) The proposed simple mechanical formula was proved to provide a conservative estimate of the separation distance even though it does not consider dynamic amplification. Apparently, the assumption of sudden reversal of the direction of velocity is conservative enough to cover for possible dynamic amplification. The values predicted by the formula are small enough in absolute terms no matter they can be an order or two bigger than numerical results.

References

1) Beppu M., Kozuki S., Ishikawa N. and Miyamoto A., Experimental study on circumferential crack pattern in RC bridge piers by an impulsive push-up device, *Journal of JSCE*, No. 577/I-41, pp.165-180, 1997

2) Mori M., Ishikawa N., Suzuki K., and Masada N., Experimental study on local buckling of deformed steel pipe subjected to impulsive push-up force, *Proc. 28th Tech. Res. Symp. Kanto Branch*, I-35, pp.70-71, 2001

3) Hakuno M., Recorded Large Acceleration of Earthquake and Recorded Damage, *Proc. 26th JSCE Earth. Eng. Symp. Panel Discussion*, pp.99-102, 2001

4) Izumi H., Missed Quasi-Impact Earthquakes, *Proc. 26th JSCE Earth. Eng. Symp. Panel Discussion*, pp.103-106, 2001

5) Sonoda K., Takada N., Kobayashi Y., Takahashi K., Sugano H., Yohochi N and Nakahara H., Verification of impulsive wave from viewpoint of jumping phenomena during the 1995 Hyogoken-Nanbu earthquake, *5th Simp. on Shock Problems of Struct.*, JSCE, pp.1-6, 2000

6) Ivanov R., *Failure Analysis of Structures by the Three Dimensional Discrete Element Method*, Ph.D. Thesis, Kobe University, 2001

(Received September 14,2001)